Journal of Materials and Environmental Sciences
ISSN : 2028-2508

J. Mater. Environ. Sci., 2017 Volume 8, Issue 11, Page 3921-3931

http://www.jmaterenvironsci.com/

Thermodynamic study of corrosion inhibition of carbon steel in acidic solution by new pyrimidothiazine derivative

M. Larouj[1], K. Ourrak[2], M. El M'Rabet[3], H. Zarrok[1], H. Serrar[4], M. Boudalia[5], S. Boukhriss[4], I. Warad[6], H. Oudda[1*], R. Touir[7,8]

[1] *Laboratory separation processes, Faculty of Science, University Ibn Tofail PO Box 242, Kenitra, Morocco.*
[2] *Laboratory of Chemistry/Biology Applied to the Environment, Faculty of Sciences, Moulay Ismail University, BP 11201-ZItoune, Meknès, 50070, Morocco.*
[3] *Département DSFA, Unité de chimie, Institut Agronomique et Vétérinaire Hassan II. Rabat, Morocco.*
[4] *Laboratory of Organic Synthesis, Organometallic and Theoretical, Faculty of Sciences, University Ibn Tofail, Kenitra, Morocco.*
[5] *Laboratory of Electrochimistry, Corrosion and Environment, Faculty of science, Rabat, Morocco.*
[6] *Department of Chemistry, AN-Najah National University P.O. Box 7, Nablus, Palestine.*
[7] *Laboratory of Materials Engineering and Environment: Modeling and Application, Faculty of Science, Ibn Tofail University, PO Box 133, 14000, Kenitra, Morocco.*
[8] *Regional center of education and training (CRMEF), Avenue Allal al-Fassi, Madinat Al Irfane PO Box 6210, Rabat, Morocco.*

Received 22 Feb 2017,
Revised 18 Jul 2017,
Accepted 20 Jul 2017

Keywords

- ✓ Corrosion inhibition;
- ✓ HCl;
- ✓ Pyrimidothiazine derivative;
- ✓ Weight loss method;
- ✓ Thermodynamic proprieties
- ✓ SEM analysis

H. Oudda
ouddahassan@gmail.com

Abstract

The new synthesized pyrimidothiazine derivative namely Ethyl2-(4-chlorophenyl)-6-(3,4-dimethoxyphenyl)-3-hydroxy-8-methyl-4-oxo-4,6dihydro pyrimido [2,1-b][1,3]thiazine-7-carboxylate (PTz3) as carbon steel corrosion inhibitor in molar hydrochloric acid, was studied by weight loss measurment and scanning electron microscopy (SEM). The obtained results revealed that the inhibition efficiency of PTz3 increases with increasing concentration but decreases relatively with temperature and its value reaches 82.12 % at 333 K at 5×10^{-3} M. The inhibition was assumed to occur via adsorption of the pyrimidothiazine molecules on metallic surface according to Langmuir adsorption isotherm. Both kinetic and thermodynamics parameters were calculated and discussed. SEM analysis revealed that the addition of inhibitor retards the corrosion processes, where the grain boundary attacks were completely hindered by the adsorbed inhibitor molecules.

1. Introduction

The metal corrosion in the presence of inhibitor involved many changes occurring on its surface, such as rapid etching and desorption of the inhibitor and the inhibitor itself, in some cases, may undergo decomposition and/or rearrangement [1]. Most of the effective inhibitors used contain heteroatom such as O, N, S and multiple bonds in their molecules that they are adsorbed on the metallic surface [2-12]. Therefore the effect of temperature on the inhibited acid-metal reaction is highly complex. So, this study facilitates the determination of many thermodynamic functions for the inhibition and/or the adsorption processes which contribute in determining the adsorption type of inhibitors.

Temperatures effects on acidic corrosion, most often in hydrochloric, phosphoric and sulphuric acids, have been the object of a large number of investigations [13-23]. It is generally assumed that in acid corrosion the inhibitors adsorb on the metal surface, resulting in a structural change of the double layer and reduced rate of the electrochemical partial reaction. Temperature dependence of the inhibitor efficiency and the comparison of the

activation energy values (E_a) of the corrosion process both in the absence and in the presence of inhibitors lead to some conclusions concerning the mechanism of the inhibiting action [24-27].
The aim of this paper is to study the temperature effects on carbon steel corrosion in 1 M HCl solution in the absence and presence of various concentrations of pyrimidothiazine by using gravimetric measurements and SEM analysis. Various Kinetic and thermodynamic parameters of corrosion processs were estimated and discussed.

2. Experimental details

2.1. *Compound synthesis*

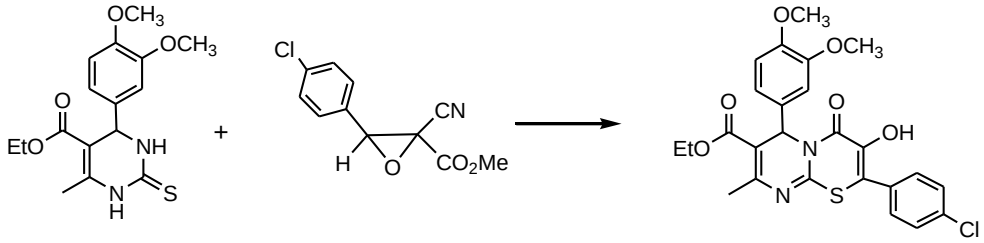

To a solution of epoxide (1 mmol) in acetonitrile (20 mL), pyrimidin-4-one (1 mmol) was added and the mixture was refluxed for 3h. The reaction mixture was distilled using rotary vacuum evaporator to afford crude product which was treated with a mixture of ether/petroleum ether, the 3-hydroxy pyrimido[2,1-b][1,3]thiazine precipitate and was recrystallized from EtOH.

2.2. Materials and solutions

The steel samples used in this study are made of carbon steel (Euronorm: C35E carbon steel and US specification: SAE 1035) with a chemical composition (in wt.%) of 0.370 % C, 0.230 % Si, 0.680 % Mn, 0.016 % S, 0.077 % Cr, 0.011 % Ti, 0.059 % Ni, 0.009 % Co, 0.160 % Cu and the remainder iron (Fe). These samples were pre-treated prior to the experiments by grinding with emery paper SiC (120, 600 and 1200); rinsed with distilled water, degreased in acetone in an ultrasonic bath immersion for 5 min, washed again with bidistilled water and then dried at hot temperature. The acids solutions (1.0 M HCl) were prepared by diluting a reagent of analytical grade HCl 37 % with double-distilled water. The concentration range of the pyrimidothiazine derivative employed was 1×10^{-4} M to 5×10^{-3} M. The molecular formula of the pyrimidothiazine derivative is shown in Figure 1.

Figure 1: Molecular formula of Ethyl2-(4-chlorophenyl)-6-(3,4-dimethoxyphenyl)-3-hydroxy-8-methyl-4-oxo-4,6dihydropyrimido [2,1-b][1,3] thiazine-7-carboxylate **(**PTz3**)**

2.3. *Weight loss measurements*

Coupons were cut into 2 cm × 2 cm × 0.08 cm dimensions are used for weight loss measurements. The electrode surface was mechanically abraded by different grades of emery papers, washed with distilled water, cleaned with acetone after being weighed accurately with high sensitivity balance, the specimens were carried out in a double glass cell equipped with a thermostated cooling condenser containing 80 mL of non-de-aerated test solution with and without various concentrations of the studied pyrimidothiazine compound (PTz3) at different temperatures range (303-333 K). After immersion period, the specimens were taken out, rinsed thoroughly with bidistilled water, dried and weighed accurately again. In order to get good reproducibility, parallel triplicate experiments were performed and the average weight loss value of three parallel carbon steel sheets was obtained. The corrosion rate (C_R) was calculated by the following equation (1):

$$C_R = \frac{\Delta m}{St} \quad (1)$$

Where C_R is the corrosion rate in (mg cm^{-2} h^{-1}), Δm is the average weight loss of three parallel carbon steel sheets (mg), S is the total area of one carbon steel sheet (cm^2), and t is the immersion time (h).

With the calculated corrosion rate, the inhibition efficiency $\eta_w(\%)$ was obtained as the following equation (2):

$$\eta_w(\%) = \frac{C_R - C_{R(inh)}}{C_R} \times 100 \quad (2)$$

Where C_R and $C_{R(inh)}$ represent the corrosion rates in the absence and presence of PTz3, respectively.

2.4. *Scanning electron microscopy*

Immersion corrosion analysis of carbon steel samples in the acidic solutions without and with the optimal concentration of the inhibitor PTz3 was performed using SEM. After elapsed time (6h) carbon steel specimens were taken out and cleaned with double distilled water, dried with cold air blower and finally the scanning electron microscopy micrographs were recorded using SEM model Quanta 200 FEI Scanning instrument at an accelerating voltage of 20kV at 5000×magnification.

3. Resulats and Discussion

3.1. Effect of PTz3 on the corrosion rate of carbon steel at various temperatures

The temperature effect on the performance of PTz3 at its various concentration in the temperature domain (303-333 K) at 6 h of immersion. The obtained results are given in Table 1. It is remarked that the inhibition efficiency decreases with increasing temperature indicating that higher temperature dissolution of carbon steel predominates on adsorption of PTz3 molecules at the mettalic surface.

Table 1: Inhibition efficiencies and corrosion rate for different concentrations of PTz3 in 1 M HCl at different temperatures.

T (K)	Conc. (M)	C_R (mg/cm^2 h)	η_w (%)	θ
303	5×10^{-3}	0.055	95	0.95
	1×10^{-3}	0.075	93	0.93
	5×10^{-4}	0.094	92	0.92
	1×10^{-4}	0.129	89	0.89
313	5×10^{-3}	0.169	93	0.93
	1×10^{-3}	0.226	91	0.91
	5×10^{-4}	0.323	87	0.87
	1×10^{-4}	0.479	81	0.81
323	5×10^{-3}	0.552	89	0.89
	1×10^{-3}	0.727	86	0.86
	5×10^{-4}	1.164	77	0.77
	1×10^{-4}	1.784	65	0.65
333	5×10^{-3}	1.793	82	0.82
	1×10^{-3}	2.679	73	0.73
	5×10^{-4}	3.484	65	0.65
	1×10^{-4}	4.866	52	0.52

3.2. Thermodynamic activation functions of the corrosion process

In order to calculate activation thermodynamic parameters of the corrosion reaction such as activation energy E_a^*, activated entropy ΔS_{ads}^* and enthalpy ΔH_a^*, the Arrhenius equation and its alternative formulation called transition state equation were employed [28]:

$$C_R = k \exp\left(\frac{-E_a^*}{RT}\right) \quad (3)$$

$$C_R = \frac{RT}{Nh}\exp\left(\frac{\Delta S_a^*}{R}\right)\exp\left(-\frac{\Delta H_a^*}{RT}\right) \quad (4)$$

where C_R is the corrosion rate, k is a constant depends on a metal type and electrolyte, E_a^* is the apparent activation energy, h is the Planck's constant (6.626176×10^{-34} J s), N is the Avogadro's number (6.02252×10^{23} mol^{-1}), R is the universal gas constant and T is the absolute temperature, ΔH_a^* is the enthalpy of activation, and ΔS_a^* is entropy of activation.

Arrhenius plots of the logarithm of the corrosion rate obtained by weight loss measurement versus 1/T for blank solution and different concentrations of PTz3 were shown in Figure 2. The process of adsorption between the metal surface and the inhibitor can sometimes be an exothermic process where the heat is given off, although in some cases, endothermic process is encountered.

It was clear that the E_a^* values in the presence of PTz3 are higher than this in the blank solution. These results are in accord with the reported studies [29,30]. The increase in the apparent activation energy E_a^* at low inhibitor concentrations (Table 2), may be interpreted as physical adsorption that occurs in the first stage [31,32]. According to equation (3), it is clear that the lower k and the higher E_a^* lead to the lower corrosion rate (C_R). For the present study, the value of k in the presence of PTz3 is higher than that in blank solution and so the decrease in carbon steel corrosion rate is determined by the apparent activation energy (E_a^*).

The enthalpy ΔH_a^* and ΔS_a^* of activation values were obtained from the transition state Eq. (4). A plot of Ln (C_R/T) as a function of 1/T (Figure 2) was made for carbon steel corrosion in 1 M HCl in the absence and presence of different concentrations of PTz3. Straight lines are obtained with a slope ($-\Delta H_a^*/R$) and intercept (Ln R/Nh + $\Delta S_a^*/R$) from which the ΔH_a^* and ΔS_a^* values are calculated (Table 2).

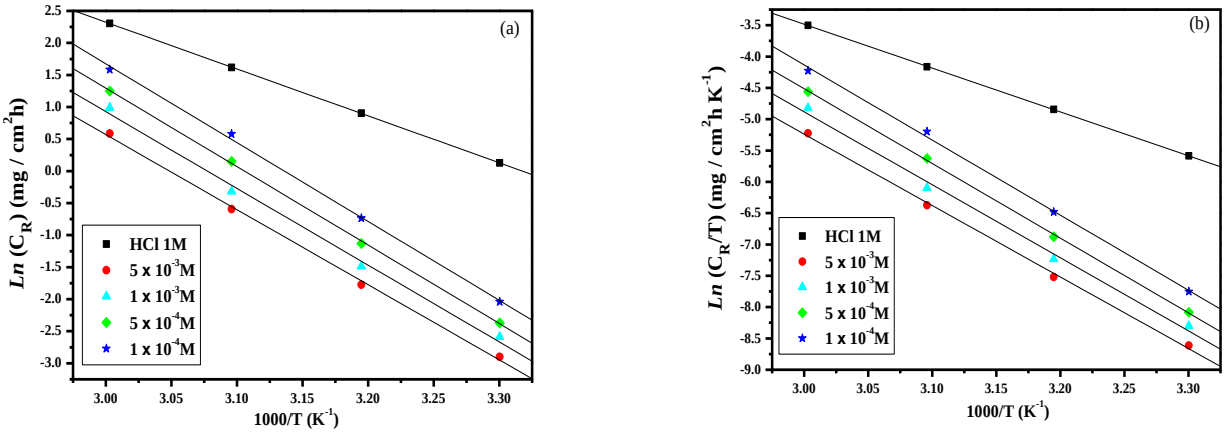

Figure 2: (a) Arrhenius plots (b) Transition state plots for the carbon steel in 1 M HCl in the absence and presence of different concentrations of PTz3 at different temperatures of PTz3 in 1.0 HCl

In addition, it is seen that the values of ΔH_a^* and ΔS_a^* in the presence of the additives increase over that of the uninhibited solution. This implies that energy barrier of the corrosion reaction in the presence of PTz3 increases which is expected. The positive values of ΔH_a^* show the endothermic nature of the dissolution process. The large negative value of ΔS_a^* for carbon steel in 1 M HCl implies that the activated complex is the rate-determining step, rather than the dissociation step. In the presence of the inhibitor, the value of ΔS_a^* increases and is generally interpreted as an increase in disorder as the reactants are converted to the activated complexes

[33]. The positive values of ΔS_a^* reflect the fact that the adsorption process is accompanied by an increase in entropy, which is the driving force for the inhibitor adsorption onto the carbon steel surface.

Table 2: Some activation parameters as function of PTz3 concentration

Conc. (M)	(k) (mg/cm^2 h)	Linear regression coefficient (r^2)	E_a^* (kJ/mol)	ΔH_a^* (kJ/mol)	ΔS_a^* (J/mol K)	$E_a^* - \Delta H_a^*$ (kJ/mol)
Blank	3.4794×10^{10}	0.99996	60.83	58.19	-91.95	2.64
1×10^{-4}	5.7406×10^{16}	0.99780	102.30	99.66	67.07	2.64
5×10^{-4}	3.2814×10^{16}	0.99941	101.81	99.17	62.42	2.64
1×10^{-3}	$.0188\times10^{16}$	0.99333	99.58	96.94	52.69	2.64
5×10^{-3}	3.4319×10^{15}	0.99771	97.48	94.84	43.43	2.64

The relationship between the activation energy E_a^* against the PTz3 concentration is shown in Figure 3. From the data reported in Table 2, it seems that (E_a^*) decreases with the concentration of inhibitor. This result permits to verify the known thermodynamic relation between (E_a^*) and ΔH_a^* as shown also in Table 2:

$$E_a^* - \Delta H_a^* = RT \qquad (5)$$

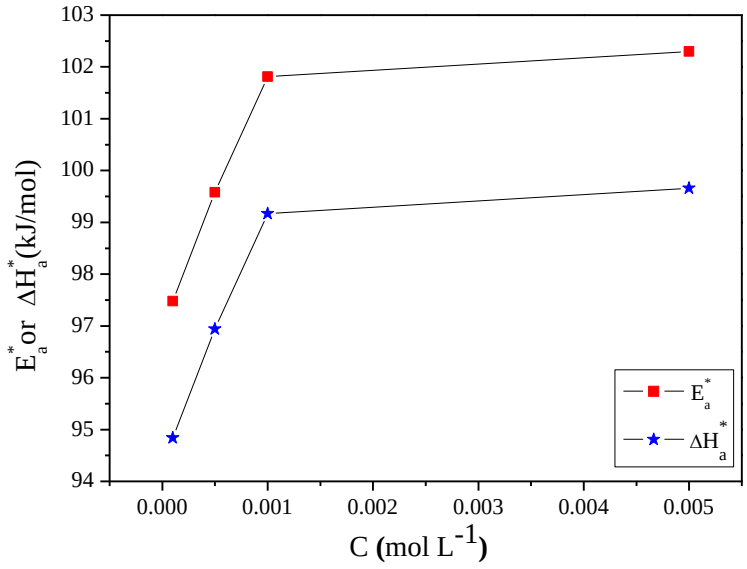

Figure 3: The relationships between (E_a^*) and ΔH_a^* with concentration of PTz3

3.3. Effect of immersion time

We conducted this study for not to confuse between the inhibition rate of the inhibitors and the passivation phenomenon which could happen if the dive time is very long. Figure 4a shows the variation of the weight loss of carbon steel in 1 M HCl and without and with 5×10^{-3} M of PTz3, during an immersion time between 4 h and 24 hours. It is noted that the obtained curves are almost linear; this implies that the surface of metals is devoid of insoluble corrosion products [20]. The relatively large divergence of plots indicates the increase of $\eta_w(\%)$ with time as shown in Figure 4b. It is noteworthy that the inhibition efficiency attains 96.2 % since 8 h and decreases slightly to 93.3 % at 24 h at 303 K. This result promises also the use of PTz3 even during a long period. So we can deduce the immersion time is not a striking effect on the performance of this inhibitor.

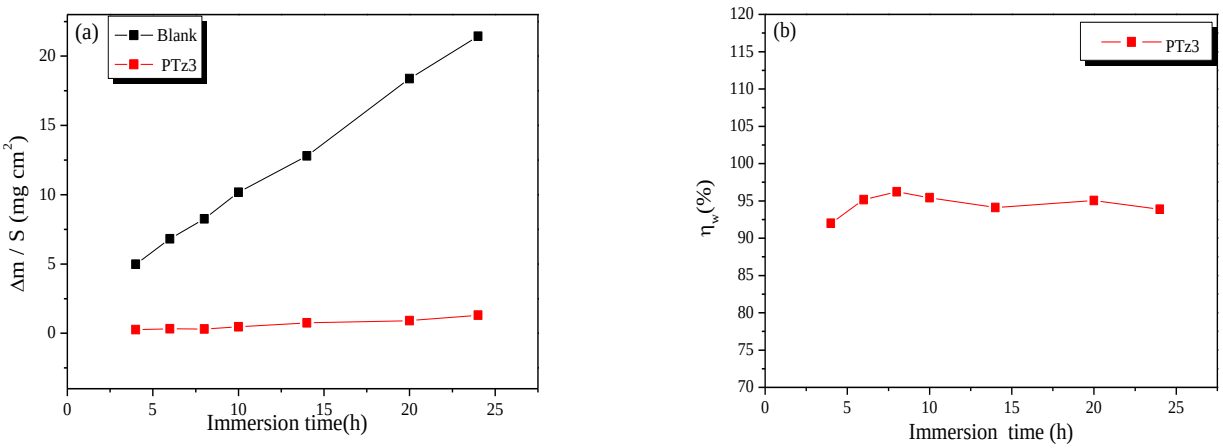

Figure 4: (a) Weight loss and **(b)** $\eta_w(\%)$ versus immersion time of carbon steel in 1 M HCl without and with 5×10^{-3} M of PTz3 at 303 K

3.4. Adsorption isotherm and thermodynamic parameters

The adsorption behavior of the inhibitor molecules on metal surface explains their inhibition mechanism [34,35]. Several adsorption isotherms can be used to assess the adsorption behavior of the inhibitors. Langmuir adsorption isotherm is the best description of the adsorption behavior of the inhibitor molecules on the carbon steel surface, which obeys Eq. (6) as follows [36,37]. The values of surface coverage (θ) for different concentrations have been used to explain the best isotherm that determines the adsorption process. The surface coverage values (θ) were evaluated using corrosion rate values obtained from the weight loss method. Coverage can be obtained from weight loss measurement by the following equation: $\theta = \dfrac{C_R - C_{R(inh)}}{C_R}$ (6)

Attempts were made to fit θ values to various isotherms including Langmuir, Frumkin, Temkin and Flory-Huggins isotherms as follows [38-41] :

Langmuir $$\frac{C}{\theta} = \frac{1}{K} + C \quad (7)$$

Temkin $$\exp(f\theta) = KC \quad (8)$$

Frumkin $$\left(\frac{\theta}{1-\theta}\right)\exp(-2f\theta) = KC \quad (9)$$

Flory-Huggins $$Log\left(\frac{\theta}{C}\right) = Log(K) + a(1-\theta) \quad (10)$$

θ is the surface coverage, K is the adsorption-desorption equilibrium constant, *C* is the concentration of inhibitor and *f* is the factor of energetic inhomogeneity.

The corresponding plots are shown in Figure 5. The values of R^2 for the PTz3 inhibitor at different adsorption isotherms are recorded in Table 3. From These results, it is concluded that Langmuir isotherm shows the best correlation with the experimental data.

The values of K_{ads} can be calculated at each studied temperature from the intercept of the straight lines in Langmuir plots. The K_{ads} related to the standard free energy of adsorption ΔG^*_{ads} by following Eq. (11) :

$$\Delta G^*_{ads} = -RTLn(55.5K_{ads}) \quad (11)$$

Where R is the universal gas constant, J mol^{-1} K^{-1}, the value of 55.5 is the concentration of water in acid solution in mol/L [42] and T is the absolute temperature. The values of K_{ads} and ΔG^*_{ads} are summarized in Table 4.

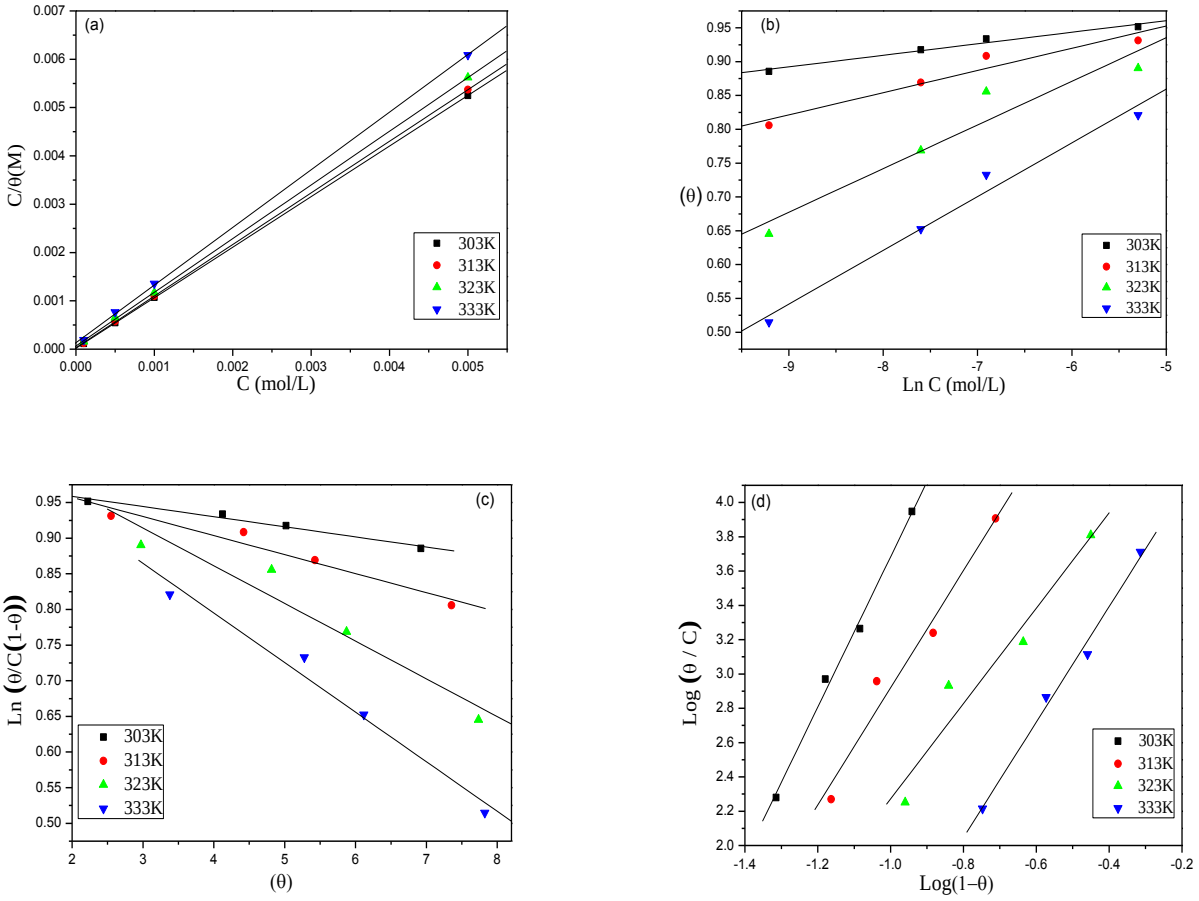

Figure 5: (a) Langmuir, (b) Temkin, (c) Frumkin and (d) Flory-Huggins isotherms for the adsorption of pyrimidothiazine derivative on the surface of carbon steel in 1 M HCl

Table 3: The values of linear regression coefficient (r^2) for the PTz3 at different adsorption isotherms

T (K)	Langmuir Isotherm	Temkin Isotherm	Frumkin Isotherm	Flory-Huggins Isotherm
303	0.99999	0.96081	0.96308	0.99105
313	0.99997	0.90903	0.92384	0.95287
323	0.99989	0.87938	0.89834	0.91097
333	0.99957	0.97236	0.96386	0.98692

Adsorption equilibrium constants K_{ads} and other thermodynamic parameters for the adsorption process are listed in Table 4. A high value of K_{ads} indicates that the inhibitors are easily and strongly adsorbed on the metal surface, mean better inhibition efficiency of the inhibitor. The calculated values of ΔG^*_{ads} using Eq. (11) are between -35.75 and -37.78 kJ/mol. In general, the adsorption of organic molecules on metal surfaces is considered as physisorption when the absolute value of ΔG^*_{ads} is 20 KJ/mol or lower. When the absolute value of ΔG^*_{ads} is 40 KJ/mol or higher, the adsorption is considered to be chemisorptions, this process, involve charge sharing or transfer of electrons from the inhibitor molecules to the metal surface to form a coordinate type bond [43]. According to the obtained values of ΔG^*_{ads}, it can be suggested that the interaction of the PTz3 involves both physisorption and chemisorptions [44].

The corrosion inhibition of PTz3 for carbon steel may be well explained by using a thermodynamic model, so, the enthalpy, the free energy and the entropy of adsorption are calculated to elucidate the phenomenon for the inhibition action of PTz3.

The enthalpy and entropy of adsorption ΔH^*_{ads} and ΔS^*_{ads} can be calculated using the Van't Hoff equation [45,46]:

$$LnK_{ads} = -\frac{\Delta H^*_{ads}}{RT} + \frac{\Delta S^*_{ads}}{R} - Ln(55.5) \quad (12)$$

Using Eq. (12), the values of ΔH^*_{ads} and ΔS^*_{ads} were evaluated from the slope and intercept of the plot of Ln (K) versus 1/T (Figure 6). The values of ΔH^*_{ads} and ΔS^*_{ads} are given in Table 4.

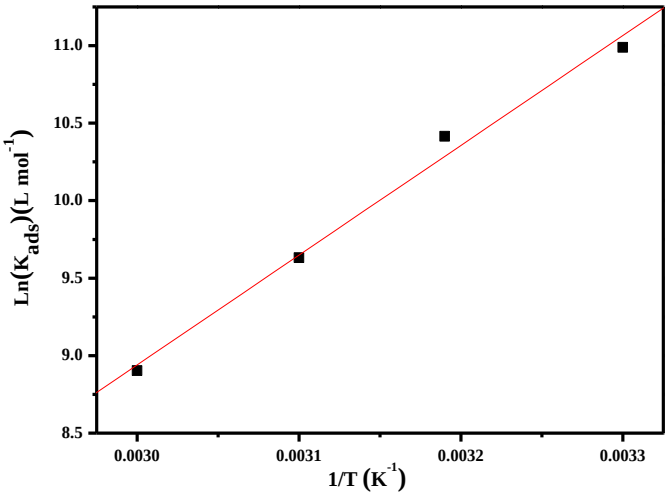

Figure 6: The relationship between Ln (K_{ads}) and 1/T

Table 4: The thermodynamic parameters of adsorption of PTz3 molecules on the carbon steel surface

Temp (K)	Langmuir adsorption isotherm			Van't Hoff equation	
	Linear regression coefficient (r^2)	K_{ads} (L/mol)	ΔG^*_{ads} (kJ/mol)	ΔH^*_{ads} (kJ/mol)	ΔS^*_{ads} (J/K mol)
303	0.99999	59234	-37.80	-58.94	-69.16
313	0.99997	33367.6	-37.56		
323	0.99989	15245.6	-36.65		
333	0.99957	7358.4	-35.77		

Further valuable information regarding the adsorption of PTz3 molecules on the carbon steel surface and the mechanism of corrosion inhibition can be provided through inspection of the values of enthalpy and entropy of adsorption. The negative value of entropy of adsorption shows that the destruction on the metal surface has been lowered and the positive once shows that the disordering of the system has increased [47]. Enthalpy values can present both the endothermic or exothermic reaction depending on the sign of the value. Moreover endothermic processes are related to chemical adsorption while exothermic processes are related to either chemical or physical adsorption [48,49]. Chemical adsorption is the most preferred over physical if prolonged results are desired. This is due to the fact that chemical adsorption is related to the sharing of electron pairs between the inhibitors and the empty of unpaired d-orbitals of the metals whereas physical adsorption is related to the

electrostatic interactions between charged inhibitor molecules and the charged surfaces of the metals. Literature shows that by considering the absolute value of ΔH^*_{ads} an exothermic process can further be classified as either chemical adsorption or physical adsorption. The values of ΔH^*_{ads} lower than 40 kJ mol^{-1} are characterized with physical adsorption while those around 100 kJ mol^{-1} or more are characterized with chemical adsorption [50,51]. Careful inspection of Table 3 shows that ΔH^*_{ads} values are negative, hence an exothermic process. The magnitudes of the absolute values of ΔH^*_{ads} for our inhibitor used is above the 40 kJ mol^{-1} thres hold and yet less than 100 kJ mol^{-1} signifying a mixed-type adsorption nature with predominance of chemisorption.

The enthalpy of adsorption found by the Van't Hoff equation may be also evaluated by the Gibbs-Helmholtz equation, which is defined as follows:

$$\frac{\Delta G^*_{ads}}{T} = \frac{\Delta H^*_{ads}}{T} - \Delta S^*_{ads} \qquad (13)$$

The variation of ΔG^*_{ads}/T with 1/T gives a straight line with a slope that equals ΔH^*_{ads} = -58.93 kJ mol^{-1} and intercept equals ΔS^*_{ads} = -69.18 J mol^{-1} K^{-1} (Fig. 7). It can be seen from the Figure that ΔG^*_{ads}/T decreases with 1/T. The value of the enthalpy of adsorption found by the two methods, Van't Hoff and Gibbs-Helmholtz relations, are in good agreement.

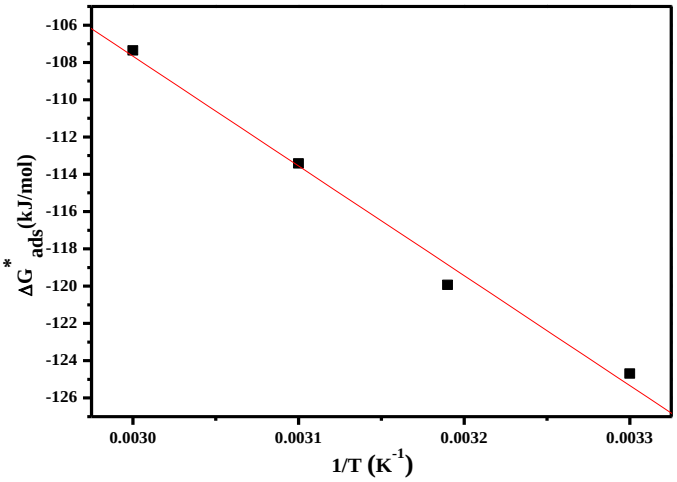

Figure 7: The relationships between ΔG^*_{ads} /T and 1/T

3.5. SEM analysis of metal surface

Scanning electron micrographs of the carbon steel surface before and after of the immersion in 1 M HCl with and without addition of PTz3 were taken in order to establish whether inhibition is due to the formation of an organic film on the metal surface. The obtained micrographs are presented in Figure 8. Parallel features on the polished carbon steel surface before exposure to the corrosive solution were observed in Figure 8a, which are associated with polishing scratches. Figure 8b and 8c show the carbon steel surface after 6 h of immersion in 1 M HCl without and with 5×10^{-3} M of PTz3. The resulting of the high resolution SEM micrograph (Figure 8b) shows that the carbon steel surface was strongly damaged in the absence of the PTz3 with the increased number and depth of the pits. However, there are less pits and cracks observed in the micrographs in the presence of PTz3 (Figure 8c) which suggests a formation of protective film on carbon steel surface which was responsible for the corrosion inhibition. Indeed, PTz3 has a strong tendency to adhere to the metallic surface and can be regarded as good inhibitor for carbon steel corrosion in normal hydrochloric medium. The high inhibitive performance of this pyrimidothiazine derivative suggests a strong bonding of the PTz3 on the metal surface due to presence of lone pairs from heteroatom (nitrogen, oxygen and sulfur) and π-orbitals, blocking the active sites and therefore decreasing the corrosion rate.

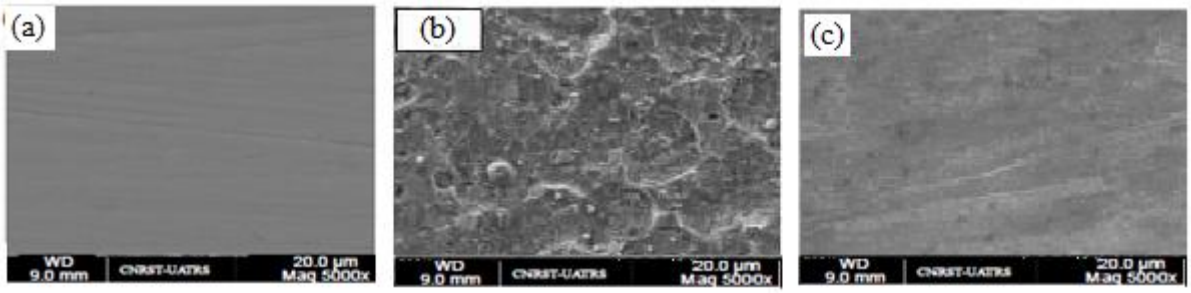

Figure 8: SEM micrographs of carbon steel : (a) unexposed, (b) exposed in 1 M HCl and (c) exposed in 1 M HCl in the presence of 5×10^{-3} M of PTz3 at 303 K

Conclusions

The Ethyl 2-(4-chlorophenyl)-6-(3,4-dimethoxyphenyl)-3-hydroxy-8-methyl-4-oxo-4,6dihydroprimido[2,1-b] [1,3]thiazine-7-carboxylate (PTz3) presents good effectiveness in 1 M HCl and even at higher temperature. The Inhibition efficiency increases with rise of concentration and decreases with temperature. Adsorption of inhibitor tested fellows Langmuir adsorption isotherm. Taking into account the increase of both activation energy and pre-exponential factor for the kinetic process of iron dissolution and the values of Gibbs free energy and heat energy for thermodynamic process of PTz3 adsorption on carbon steel surface, the authors believe that the adsorption mechanism of PTz3 may be a combination of both chemisorption and physisorption. The SEM results showed that the inhibition effect is more pronounced in the presence of this pyrimidothiazine.

References

1. Barsoukov E., Macdonald J., John Wiley & Sons: Hoboken, 2005.
2. Ghazoui A., Saddik R., Benchat N., Hammouti B., Guenbour M., Zarrouk A., Ramdani M., *Der Pharm. Chem.* 4 N°1 (2012) 352.
3. Zarrok H., Saddik R., Oudda H., Hammouti B., El Midaoui A., Zarrouk A., Benchat N., Ebn Touhami M., *Der Pharm. Chem.* 3N°5 (2011) 272.
4. Zarrouk A., Hammouti B., Touzani R., Al-Deyab S.S., Zertoubi M., Dafali A., Elkadiri S., *Int. J. Electrochem. Sci.* 6 (2011) 4939.
5. Zarrouk A., Hammouti B., Dafali A., Zarrok H., *Der Pharm. Chem.* 3 N°4 (2011) 266.
6. Ghazoui A., Zarrouk A., Bencaht N., Salghi R., Assouag M., El Hezzat M., Guenbour A., Hammouti B., *J. Chem. Pharm. Res.* 6 (2014) 704.
7. Zarrok H., Zarrouk A., Salghi R., Oudda H., Hammouti B., Assouag M., Taleb M., Ebn Touhami M., Bouachrine M., Boukhris S., *J. Chem. Pharm. Res.* 4N°12 (2012) 5056.
8. Zarrok H., Zarrouk A., Salghi R., Assouag M., Hammouti B., Oudda H., Boukhris S., Al Deyab S.S., Warad I., *Der Pharm. Lett.* 5N°2 (2013) 43.
9. Belayachi M., Serrar H., Zarrok H., El Assyry A., Zarrouk A., Oudda H., Boukhris S., Hammouti B., Ebenso E.E., Geunbour A., *Int. J. Electrochem. Sci.* 10 (2015) 3010.
10. Zarrouk A., Zarrok H., Salghi R., Touir R., Hammouti B., Benchat N., Afrine L.L., Hannache H., El Hezzat M., Bouachrine M., *J. Chem. Pharm. Res.* 5N°12 (2013) 1482.
11. Zarrok H., Zarrouk A., Salghi R., Ebn Touhami M., Oudda H., Hammouti B., Touir R., Bentiss F., Al-Deyab S.S., *Int. J. Electrochem. Sci.* 8 (2013) 6014.
12. Ben Hmamou D., Aouad M.R., Salghi R., Zarrouk A., Assouag M., Benali O., Messali M., Zarrok H., Hammouti B., *J. Chem. Pharm. Res.* 4 (2012) 34984.
13. Abiola O., Aliyu A., Phillips A., Ogunsipe A., *J. Mater. Environ. Sci.* 4 (2013) 370.
14. Shivakumar S., Mohana K., *J. Mater. Environ. Sci.* 4 (2013) 448.
15. Hmamou D.B., Salghi R., Zarrok H., Zarrouk A., Hammouti B., El Hezzat M., Bouachrine M., *Adv. Mater. Corros.* 2 (2012) 36.
16. Akalezi C.O., Enenebaku C.K., Oguzie E.E., *J. Mater. Environ. Sci.* 4 (2013) 217.
17. Rekkab S., Zarrok H., Salghi R., Zarrouk A., Bazzi Lh., Hammouti B., Kabouche Z., Touzani R., Zougagh M., *J. Mater. Environ. Sci.* 3 (2012) 613.

18. Elbribri A., Tabyaoui M., El Attari H., Boumhara K., Simiti M., Tabyaoui B., *J. Mater. Environ. Sci.* 2 (2011) 156.
19. Benabdellah M., Touzani R., Dafali A., Hammouti B., El Kadiri S., *Mater. Lett.* 61 (2007) 1197.
20. Bouklah M., Hammouti B., Lagrenee M., Bentiss F., *Corros. Sci.* 48 (2006) 2831.
21. Obi-Egbedi N., Essien K., Obot I., Ebenso E., *Int. J. Electrochem. Sci.* 6 (2011) 913.
22. Khadom A.A.,Yaro A.S., AlTaie A., Kadum A., *Port. Electrochimica Acta.* 27 (2009) 699.
23. Larouj M., ELaoufir Y., Serrar H., El Assyry A., Galai M., Zarrouk A., *Der Pharm. Lett.* 6 N°4 (2014) 324.
24. Zarrouk A., Zarrok H., Ramli Y., Bouachrine M., Hammouti B., Sahibeddine A., Bentiss F., *J. Mol. Liq.* 222 (2016) 239.
25. Bendaha H., Zarrouk A., Aouniti A., Hammouti B., El Kadiri S., Salghi R., Touzani R., *Phys. Chem. News* 64 (2012) 95.
26. Benabdellah M., Tounsi A., Khaled K., Hammouti B., *Arab. J. Chem.* 4 (2011) 17.
27. Fu J., Pan J., Liu Z., Li S., Wang Y., *Int. J. Electrochem. Sci.* 6 (2011) 2072.
28. Hammouti B., Zarrouk A., Al-Deyab S.S., Warad I., *Orient. J. Chem.*2 7 (2011) 23.
29. Elachouri M., Hajji M.S., Salem M., Kertit S., Aride J., Coudert R., Essassi E., *Corrosion* 52 (1996) 103.
30. Ferreira E., Giacomelli C., Giacomelli F., Spinelli A., *Mater. Chem. Phys.* 83 (2004) 129.
31. Szauer T., Brandt A., *Electrochim. Acta.* 26 (1981) 1253.
32. El Sherbini E.F., *Mater. Chem. Phys.* 60 (1999) 286.
33. Ouali I. El, Hammouti B., Aouniti A., Ramli Y., Azougagh M., Essassi E., Bouachrine M., *J. Mater. Environ. Sci.* 1 (2010) 1.
34. Durnie W., Kinsella B., De Marco R., Jefferson A., *J. Appl. Electrochem.* 31 (2001) 1221.
35. Tang Y.M., Yang W.Z., Yin X.S., Liu Y., Wan R., Wang J.T., *Mater. Chem. Phys*. 116 (2009) 479.
36. Morad M., *J. Appl. Electrochem.* 38 (2008) 1509.
37. Quraishi M., Jamal D., *Mater. Chem. Phys.* 68 (2001) 283.
38. Agrawal R., Namboodhiri T., *Corros. Sci.* 30 (1990) 37.
39. Do D.D., Adsorption Analysis: Equilibria and Kinetics:(With CD Containing Computer Matlab Programs), World Scientific, 1998.
40. Zhao T., Mu G., *Corros. Sci.* 41 (1999) 1937.
41. Yaro A.S., Khadom A.A., Ibraheem H.F., *Anti-Corros. Methods Mater*. 58 (2011) 116.
42. Olivares O., Likhanova N., Gomez B., Navarrete J., Llanos-Serrano M., Arce E., Hallen J., *Appl. Surf. Sci.* 252 (2006) 2894.
43. Szklarska-Smialowska Z., Mankowski J., *Corros. Sci.* 18 (1978) 1953.
44. Yang Z., Zhan F., Pan Y., Yu Z. L., Han C., Hu Y., Ding P., Gao T., Zhou X., Jiang Y., *Corros. Sci.* 99 (2015) 281.
45. Tang L., Mu G., Liu G., *Corros. Sci.* 45 (2003) 2251.
46. Zhao T., Mu G., *Corros. Sci.* 41 (1999) 1937.
47. Behpour M., Ghoreishi S., Khayatkashani M., Soltani N., *Mater. Chem. Phys.* 131 (2012) 621.
48. Obot I.B., Ebenso E.E., Kabanda M.M., *J. Environ. Chem. Eng.* 1 (2013) 431.
49. Durnie W., De Marco R., Jefferson A., Kinsella B., *J. Electrochem. Soc.* 146 (1999) 1751.
50. Quraishi M., Singh A., Singh V.K., Yadav D.K., Singh A.K., *Mater. Chem. Phys.* 122 (2010) 114.
51. Satapathy A., Gunasekaran G., Sahoo S., Amit K., Rodrigues P., *Corros. Sci.* 51 (2009) 2848.

(2017) ; http://www.jmaterenvironsci.com